

Dielectric properties of mixtures of a bent-core and a calamitic liquid crystal

Péter Salamon, Nándor Éber, and Ágnes Buka

Research Institute for Solid State Physics and Optics, Hungarian Academy of Sciences, H-1525 Budapest, P.O. Box 49, Hungary

James T. Gleeson and Samuel Sprunt

Department of Physics, Kent State University, Kent, Ohio 44242, USA

Antal Jákli

Liquid Crystal Institute, Kent State University, Kent, Ohio 44242, USA

(Received 29 September 2009; revised manuscript received 7 January 2010; published 24 March 2010)

Dielectric spectroscopy measurements have been performed on a bent-core nematic liquid crystal and on its binary mixtures with a calamitic nematic. We have detected more dispersions in the bent-core compound than in the calamitic one, including one at an unusually low frequency of a few kilohertz. The dispersions detected in the mixtures have been identified and the spectra have been split into contributions of the constituents. In order to connect the dielectric increment with the molecular dipole moment we have applied a sophisticated conformational calculation not performed before for a large, flexible mesogen molecule with numerous polar groups.

DOI: [10.1103/PhysRevE.81.031711](https://doi.org/10.1103/PhysRevE.81.031711)

PACS number(s): 77.84.Nh, 77.22.Gm, 61.30.Gd, 31.15.bu

I. INTRODUCTION

Bent core (BC) mesogens represent a relatively young family of liquid crystals. The steric interactions due to their banana shape might lead to the occurrence of phases with unique ordering like the series of “banana” phases (B_1, \dots, B_8). These include a phase with polar ordering (B_2) which is (anti)ferroelectric and is able to form chiral domains spontaneously even if the material is exclusively composed of achiral molecules [1].

Although bent-shape molecules may form columnar (B_1), smectic (B_2, B_3, B_6 and B_7) and nematic (BCN) phases, just as their calamitic counterparts, the BCN structure is much less common than the nematic (N) phase of the calamitics. This is mainly because of the kinked shape that is not really compatible with the translational freedom of the calamitic nematics. For this reason BCNs exhibit some unusual physical properties compared to calamitic ones. These include giant flexoelectricity [2], unprecedented scenarios in electroconvection [3–5], as well as an unusual behavior found by light scattering [6] and ^2H NMR measurements [7] indicating the presence of clusters with higher ordering not only in the nematic but also well in the isotropic phase.

Dielectric spectroscopy is a widespread tool for studying liquid crystals which is based on determining the frequency (f) dependent complex permittivity of the substance. It provides not only important material parameters like the static dielectric permittivity and dc electrical conductivity but it also provides information on the molecular dynamics. The number of relaxation modes is characteristic of the phase and can be associated with certain molecular rotations; the characteristic frequencies reflect how those motions are hindered. Specifically in the nematic phase of calamitic liquid crystals typically three dielectric dispersions can be detected which usually are found at high frequencies, in the megahertz–gigahertz frequency range [8].

While the relaxation phenomena in calamitic liquid crystals have been fully explored, much less is known about that

of bent-core mesogens. Moreover, previous studies on BC compounds mainly focused on the smectic and columnar banana phases, therefore dielectric spectra of BC nematics are still mostly unexplored, although recently an unusual behavior—a double sign inversion of the conductivity anisotropy in the kilohertz range—has been detected by conductivity measurements in a BC nematic implying a possibility for a dielectric relaxation at unusually low frequencies [3]. This observation inspired us to carry out precise dielectric spectroscopic investigations on a BC nematic compound. In the present paper we demonstrate that it has more distinguishable dispersions than a usual calamitic nematic, and the relaxations in all phases and orientations occur at low frequencies. Measurements have also been extended to mixtures of BC and a specifically chosen calamitic nematic. It helps to unravel the nature of the dispersions, and by varying the concentration we are able to follow the change of properties from that of a BC nematic to those of a regular calamitic nematic.

The paper is organized as follows. In Sec. II we introduce the compounds used and our experimental technique. In Sec. III we present our measurements on the BC nematic, while in Sec. IV we report on our experimental data on the mixtures. Our calculations on molecular properties are presented in Sec. V. The paper is concluded in Sec. VI with a discussion of the obtained results. In Sec. VII we summarize our present work.

II. EXPERIMENTAL

Our experiments have been carried out on a bent-core and a rod-shaped mesogen as well as on their binary mixtures. A well characterized compound, 4-chloro-1,3-phenylenebis-4[4'-(9-decenyloxy)benzoyloxy] benzoate (CIPbis10BB) [2,3,9–11] has been chosen as the bent-core component. It exhibits a monotropic nematic phase in a sufficiently wide temperature range below 100 °C. 4-n-octyloxyphenyl 4-n-

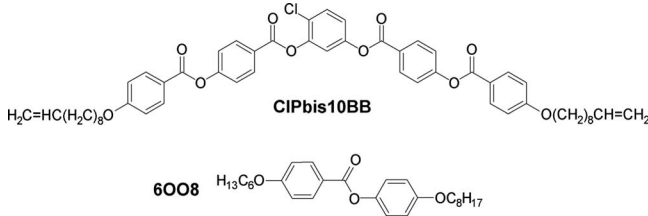


FIG. 1. Chemical structures of the bent-core CIPbis10BB and the rodlike 6OO8 molecules used in the mixtures.

hexyloxybenzoate (6OO8) has been selected as the calamitic compound, because its chemical structure is similar to that of the arms of the BC compound and has nematic and smectic-C (SmC) mesophases. The chemical schematics of both compounds are shown in Fig. 1. It has been shown recently [11] that CIPbis10BB and 6OO8 are fully miscible in their nematic phase; moreover, their mixtures exhibit a biaxial smectic phase, which most probably is an anticlinic smectic-C (SmC_A) phase. Mixtures with five different compositions have been prepared by ultrasonically dispersing the components for 30 min and keeping them at 10 °C above the highest clearing point for a day.

The dielectric studies have been carried out by using a Schlumberger 1260 impedance/gain-phase analyzer in the frequency range 200 Hz–4 MHz with the maximum applied measuring voltage of 0.1 V (RMS). For the impedance measurements a four wired configuration has been used in order to eliminate the distortive contribution of the connecting wires. To avoid high frequency distortions, the instrument has been calibrated with a 1 kΩ resistor. The dielectric properties of the substances have been investigated in custom made sandwich cells. To avoid parasitic effects, such as ITO-relaxation occurring at high frequencies, we have used gold electrodes of an area of about 6 × 6 mm² made by sputtering onto glass substrates. The electrode resistance thus could be neglected compared to the impedance of the substances. We obtained 51–54 μm thick samples by sandwiching the gold-coated glasses between nominally 50 μm thick mylar spacers. The electrodes have not been coated with any alignment layers, so the director was oriented by $B \approx 1$ T magnetic field. The compounds used have positive diamagnetic susceptibility anisotropy; hence their director aligns along the magnetic field. Rotating the cell in the magnetic field we could adjust the director either parallel or perpendicular to the electrode normals; thus we could measure both the parallel (∥) and the perpendicular (⊥) component of the uniaxially symmetric dielectric tensor of the nematic phase. Our applied magnetic field reached at least eight times the value of the Fredericksz threshold field; therefore our measured values could be regarded as a good approximation for the ∥ and ⊥ components of the complex permittivity. We note here that any imperfection in the orientation affects only the susceptibility and so the height of the absorption peaks, but does not influence the relaxation frequencies.

Due to the lack of ITO and alignment layers, a simple parallel RC equivalent circuit could be used to interpret the measured complex impedance. Measuring and comparing the impedances of empty and filled cells, the complex permittivities $\epsilon^*(f) = \epsilon'(f) - i\epsilon''(f)$ of the compounds have been deter-

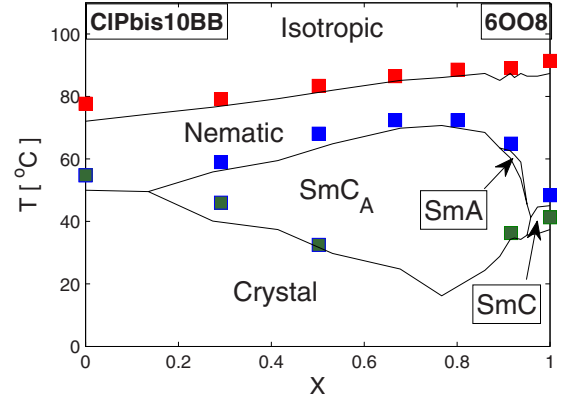


FIG. 2. (Color online) Phase transition temperatures of mixtures of different compositions in the binary system CIPbis10BB/6OO8 determined by dielectric measurements (symbols), and by polarizing microscopy [11] (solid lines). Phase identification is given according to [11].

mined. Here $\epsilon'(f)$ is the real part of the frequency dependent dielectric permittivity, $\epsilon''(f)$ is its imaginary part (the dielectric loss) and i is the imaginary unit.

The dielectric spectra of the studied substances have been analyzed by using a complex nonlinear least square (CNLS) fitting algorithm to fit the measured complex permittivity with Eq. (1), the general formula describing the complex dielectric permittivity in the presence of several dispersions,

$$\epsilon^*(f) = \epsilon(\infty) + \sum_{j=1}^k \frac{\Delta\epsilon_j}{1 + i\left(\frac{f}{f_{Rj}}\right)^{1-\alpha_j}} - i\frac{\sigma}{\epsilon_0 2\pi f}. \quad (1)$$

Here $\epsilon(\infty)$ is the high frequency limit of the dielectric permittivity, σ is the dc conductivity of the substance, ϵ_0 is the electric constant, f is the frequency, k is the number of dispersions in the dielectric frequency range ($f < 10$ GHz), while $\Delta\epsilon_j$ is the dielectric increment, f_{Rj} is the relaxation frequency and α_j is the symmetric distribution parameter of a dispersion, where $\alpha=0$ represents a simple Debye-type relaxation mode possessing a single characteristic time. On the contrary, $\alpha \neq 0$ indicates a superposition of several processes with different, though close, characteristic times.

During the measurements the cell temperatures have been kept constant within 0.1 °C precision. Temperature sweep measurements have also been performed (at 10 kHz and 0.1 V) using heating/cooling rates of 1 K/min in order to determine the phase transition temperatures. Figure 2 depicts the transition temperatures determined by this technique for all our mixtures. The results are in good agreement with the phase diagram obtained by polarizing microscopy in earlier studies on the same CIPbis10BB/6OO8 binary system [11].

III. DIELECTRIC RELAXATION IN THE PURE BENT CORE NEMATIC

The parallel and perpendicular dielectric spectra have been measured in the pure compounds as well as in the mixtures at various temperatures. For the pure BC material (CIPbis10BB) the parallel components of the permittivity ϵ_{\parallel}

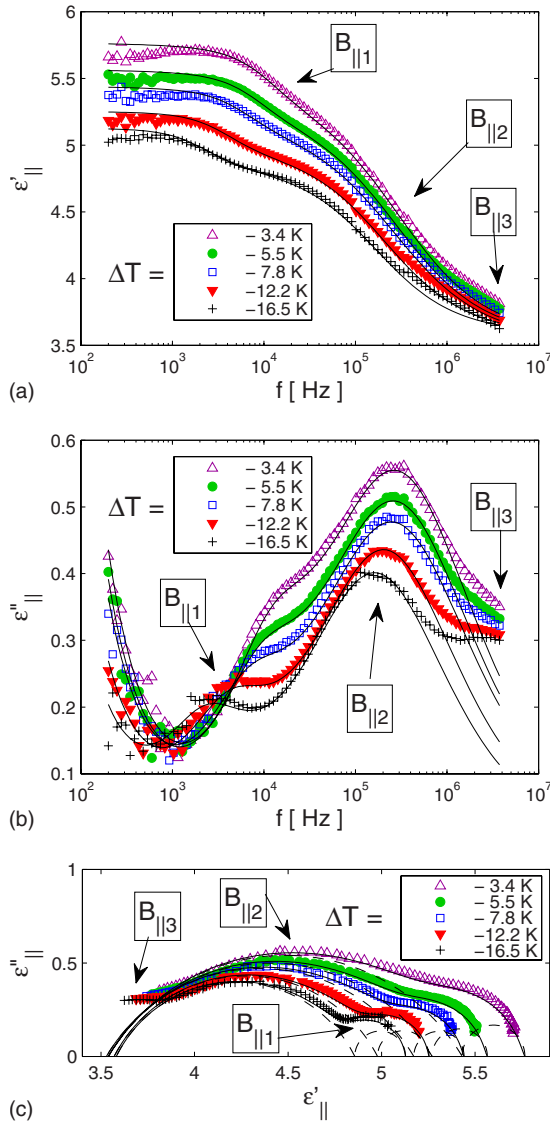


FIG. 3. (Color online) Frequency dependence of the parallel component of the (a) permittivity $\epsilon'_{||}$ and the (b) loss $\epsilon''_{||}$ in the nematic phase of CIPbis10BB at various $\Delta T = T - T_{NI}$ temperatures. (c) The corresponding Cole-Cole plot. Symbols are measured values, solid lines correspond to a fit with two relaxations. The dashed lines show the two fitted relaxations separately.

and the dielectric loss $\epsilon''_{||}$ are depicted in Figs. 3(a) and 3(b), respectively, at five different relative temperatures $\Delta T = T - T_{NI}$ in the nematic phase. Here T_{NI} corresponds to the nematic-isotropic phase transition temperature. In the frequency range studied here we can see two inflection points in the $\epsilon'_{||}(f)$ curves of Fig. 3(a) and two overlapping peaks in the loss spectra $\epsilon''_{||}(f)$ in Fig. 3(b) at the same frequencies indicating the presence of two dispersions: $B_{||1}$ at the lower (200 Hz–100 kHz) and $B_{||2}$ at the higher (100 kHz–4 MHz) part of the frequency range (from here B refers to bent-core modes). The increase of $\epsilon''_{||}(f)$ below $B_{||1}$ is due to the dc conductivity of the sample. As expected, this effect is smaller at lower temperatures. In Fig. 3(c) the real and imaginary parts of the dielectric permittivity are plotted in a Cole-Cole diagram, where the two dispersions are readily observable.

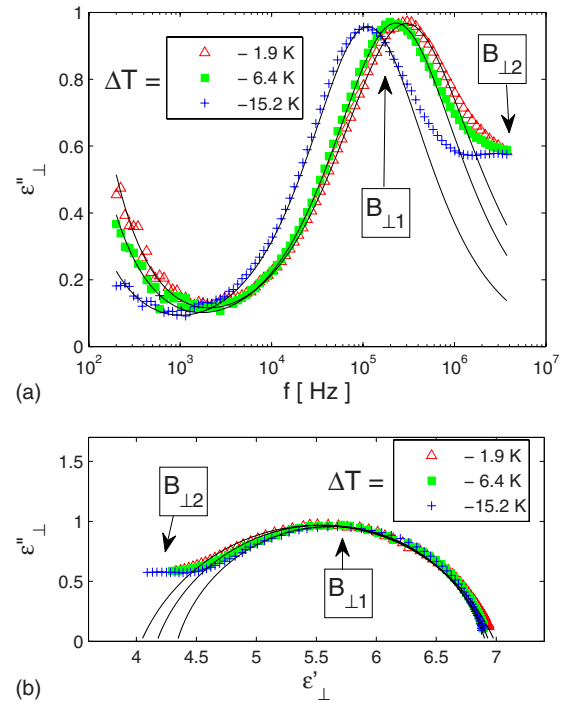


FIG. 4. (Color online) (a) Frequency dependence of the loss ϵ''_{\perp} for the perpendicular component in the nematic phase of CIPbis10BB at various $\Delta T = T - T_{NI}$ temperatures. (b) The corresponding Cole-Cole plot. Symbols are measured values, solid lines correspond to a fit with one relaxation.

In order to separate the dispersions $B_{||1}$ and $B_{||2}$, the measured complex permittivity was fitted with Eq. (1) assuming $k=2$; the solid lines in Figs. 3(a)–3(c) are the results of this fitting. Preliminary fitting results showed that $B_{||1}$ can be well described by an ideal Debye curve ($\alpha_{B||1} \approx 0 \pm 0.05$); so—for the sake of the fit’s stability—this parameter was later fixed to 0. In contrast to that, $B_{||2}$ shows $\alpha_{B||2} \approx 0.26$ – 0.31 , meaning that this is a composite dispersion consisting of different molecular processes with their characteristic frequencies close to each other. The dielectric increment of $B_{||1}$ ($\Delta\epsilon_{B||1} \approx 0.27$ – 0.36) is much smaller than that of $B_{||2}$ ($\Delta\epsilon_{B||2} \approx 1.3$ – 2.3); both weaken significantly with decreasing temperatures. [We note that all the parameters $\epsilon(\infty)$, $\Delta\epsilon$, f_R , α presented or used numerically in this paper are from fits using Eq. (1)]. The fitted curves deviate from the measured data at higher frequencies. These deviations indicate the onset of an additional, third dispersion ($B_{||3}$) at frequencies above our measurement range. The presence of the dispersion ($B_{||3}$) is corroborated by the fact that $\epsilon_{||}$ still should decrease by $\epsilon_{||}(\infty) - n_e^2 \approx 1.3$ (at $\Delta T = -13$ K) before reaching the permittivity at optical frequencies ($n_e^2 \approx 2.6$), which is too large to be covered by the infrared modes alone (infrared modes usually amount to 5%–10% of n^2 [13] in calamitics).

In Figs. 4(a) and 4(b) one can see the frequency dependence of the loss, and the Cole-Cole plot for the perpendicular component. The data clearly show only one dispersion ($B_{\perp 1}$) in the higher (100 kHz–4 MHz) part of our measurement frequency range, although a high frequency deviation from Eq. (1) with $k=1$ arises here as well. In contrast to the $B_{||2}$ dispersion, the dielectric increment of $B_{\perp 1}$ does not di-

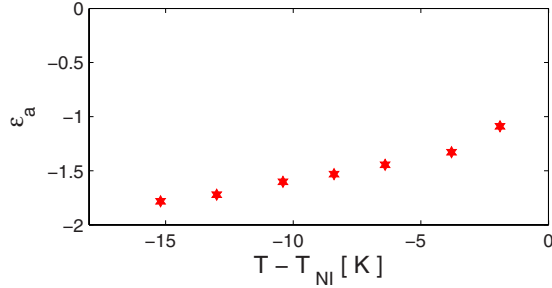


FIG. 5. (Color online) Temperature dependence of the static dielectric anisotropy (ϵ_a) in the nematic phase of CIPbis10BB.

minish significantly at decreasing temperatures. The height of the loss peak is almost twice that of $B_{\parallel 2}$. The deficiency in the dielectric increment $\epsilon_{\perp}(\infty) - n_o^2 \approx 2$ (at $\Delta T = -13$ K) here is even larger than in the \parallel component. The necessity for an additional high f relaxation ($B_{\perp 2}$) is further supported by the fact that the dielectric anisotropy ($\epsilon_a = \epsilon_{\parallel} - \epsilon_{\perp}$) of CIPbis10BB was found to be negative in the whole studied frequency range, while at optical frequencies the anisotropy is of opposite sign ($n_{\parallel} - n_{\perp} = n_e - n_o \approx 0.08 > 0$). The temperature dependence of the static dielectric anisotropy is shown in Fig. 5. We have calculated the values using the fit parameters of dielectric spectra.

Measurements have also been performed in the isotropic phase, in order to compare the molecular dipole moment and the dielectric spectra based on the existing theories. The results for the loss ϵ''_{iso} are presented in Fig. 6(a), and the corresponding Cole-Cole plots are shown in Fig. 6(b). The data display one strong dispersion (B_{iso1}) with the relaxation fre-

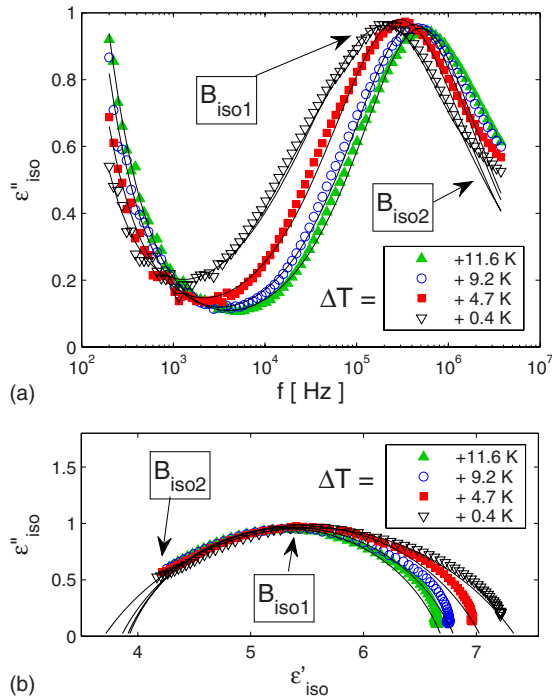


FIG. 6. (Color online) (a) Frequency dependence of the loss ϵ''_{iso} in the isotropic phase of CIPbis10BB at various $\Delta T = T - T_{NI}$ temperatures. (b) The corresponding Cole-Cole plot. Symbols are measured values, solid lines correspond to a fit with one relaxation.

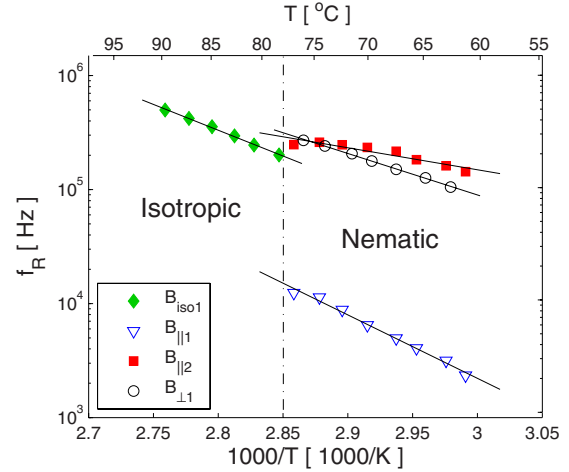


FIG. 7. (Color online) Temperature dependence of the relaxation frequencies in the isotropic and nematic phases of CIPbis10BB. Symbols are measured values, solid lines correspond to a fit to Eq. (2).

quency growing from 0.2 to 0.5 MHz, $\Delta\epsilon_{B_{iso1}}$ reducing from 3.7 to 2.8, and $\alpha_{B_{iso1}}$ changing from 0.38 to 0.23 when increasing the temperature above T_{NI} . This relaxation frequency range is unusually low for an isotropic fluid. Although the high frequency deviations from the fitted curves in Fig. 6(a) are much less pronounced here than in the nematic phase, the fairly large deficiency in the dielectric increment [$\epsilon_{iso}(\infty) - n_{iso}^2 \approx 1.4$ at $\Delta T = 5$ K] also suggests the presence of a second dispersion at higher frequencies (B_{iso2}).

The temperature dependence of the relaxation frequencies in the nematic and the isotropic phases is presented by an Arrhenius plot in Fig. 7, where the relaxation frequency f_R in logarithmic scale is plotted versus the inverse absolute temperature $1/T$. The linear dependence can be well fitted by the Arrhenius equation,

$$f_R(T) = f_0 \exp\left\{-\frac{E_A}{k_B T}\right\}. \quad (2)$$

Here f_0 is a temperature independent constant and E_A is the activation energy of the relaxation. A higher E_A may refer to a greater hindrance of the molecular process behind the dispersion. From the fit to Fig. 7 we determined the activation energies. For the B_{\parallel} dispersion E_A is found to be 1.1 eV, which counts as a relatively high value, while the activation energy corresponding to $B_{\parallel 2}$, $B_{\perp 1}$, and B_{iso1} are 0.4, 0.7, and 0.9 eV, respectively, which fall into the usual range in the corresponding phases of calamitics.

Fit parameters of the different relaxations of CIPbis10BB at the relative temperature of $\Delta T = +5$ K in the isotropic and $\Delta T = -13$ K in the nematic phase are collected in Table I. The corresponding activation energies are also shown in Table I.

IV. DIELECTRIC RELAXATIONS IN THE MIXTURES

In order to explore to what extent are the dielectric properties of our bent-core nematic different from those of a

TABLE I. The dielectric increment $\Delta\varepsilon$, relaxation frequency f_R , symmetrical distribution parameter α , asymptotic permittivity $\varepsilon(\infty)$, and activation energy E_A for the dispersions of the bent-core compound from fits in the isotropic ($\Delta T=+5$ K) and in the nematic ($\Delta T=-13$ K) phase.

Dispersions	$\Delta\varepsilon$	f_R (kHz)	α	$\varepsilon(\infty)$	E_A (eV)
B_{iso1}	3.2	310	0.3	3.8	0.9
B_{iso2}	<1.4 ($\approx \varepsilon_{iso}(\infty) - n_{iso}^2$)	>4000		$>n_{iso}^2$	
$B_{ 1}$	0.27	3.7	0		1.1
$B_{ 2}$	1.4	210	0.3	3.6	0.4
$B_{ 3}$	<1.3 ($\approx \varepsilon_{ }(\infty) - n_e^2$)	>4000		$>n_e^2$	
$B_{\perp 1}$	2.7	140	0.2	4.3	0.7
$B_{\perp 2}$	<2 ($\approx \varepsilon_{\perp}(\infty) - n_o^2$)	>4000		$>n_o^2$	

regular calamitic nematic, our studies have been extended to mixtures of the bent-core CIPbis10BB and a standard calamitic (6OO8) compound. Measurements on a binary system with full miscibility in their nematic phase [11] offered the opportunity to follow the changes in properties from a well known (calamitic) to the less explored (bent-core). In Figs. 8(a) and 8(b) the parallel components of the dielectric constant $\varepsilon'_{||}$ and the loss $\varepsilon''_{||}$ are depicted versus frequency for all the seven concentrations tested. For an adequate comparison, data for each concentration are plotted at the same relative temperature $\Delta T=-13$ K. Concentrations are given as the molar fraction X of the rodlike compound; e.g., $X=0$ refers to the pure bent-core CIPbis10BB, and $X=1$ denotes the calamitic 6OO8.

At lower frequencies ($f \sim 200$ Hz), the dielectric permittivity [Fig. 8(a)] practically equals to its static value. It changes monotonically with the concentration in the mixtures from one pure compound to the other.

Relaxation phenomena can easier be followed in looking at the absorption peaks. Figures 8(b) and 9 depict the parallel $\varepsilon''_{||}$ and the perpendicular ε''_{\perp} components of the dielectric loss versus frequency for the mixtures at the same $\Delta T=-13$ K temperature.

In order to evaluate the measurements and to separate the contributing dispersions we have applied Eq. (1) which resulted in the thin fitted lines shown in Figs. 8(b) and 9. The fitting parameters $\Delta\varepsilon$, α , and f_R , are summarized as a function of the concentration in Figs. 10(a)–10(c). The role of the lines in these figures will be discussed later.

While the pure CIPbis10BB has only a nematic mesophase, the mixtures exhibit also an induced smectic, probably anticlinic smectic-C (SmC_A) phase too [11]. The dielectric measurements have been extended to the temperature range of the SmC_A as well, in order to reveal the relationship between the relaxations observed in the different mesophases. As a representative example in Fig. 11 the frequency dependence of the loss is plotted in the SmC_A phase for both the parallel and the perpendicular components. It is seen that in the parallel case there is one strong dispersion (M_{Sml}) (M refers to the relaxations in the mixtures) with some high f deviation from the fitted curve indicating a possibility for an additional higher frequency dispersion. In the perpendicular component a very small loss peak can be de-

tected in the same frequency range as in the parallel component; it is assumed to be a crosstalk from the dispersion M_{Sml} in the parallel component. The main dispersion in the perpendicular component seems to occur outside our frequency range.

In order to compare the relaxation frequencies and their temperature dependence in the different mesophases in Fig.

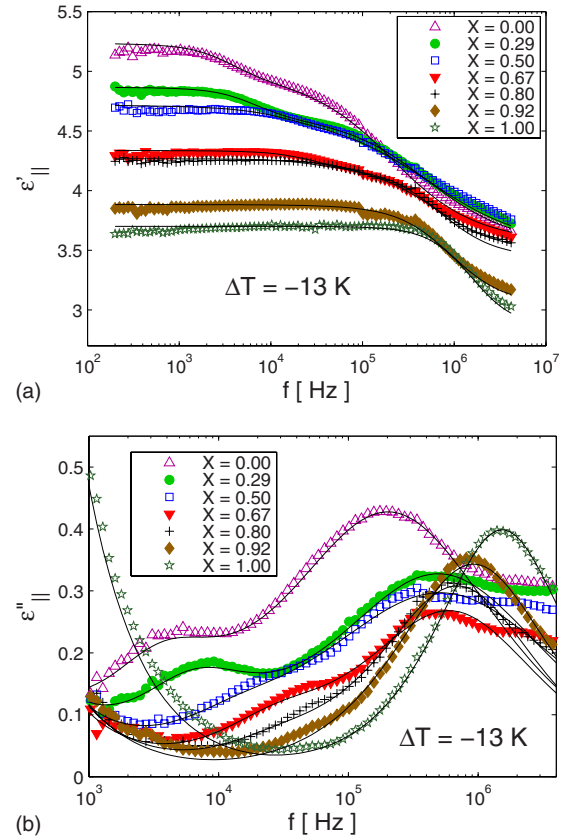


FIG. 8. (Color online) Frequency dependence of the parallel component of the (a) permittivity $\varepsilon'_{||}$ and of the (b) loss $\varepsilon''_{||}$ in the nematic phase of binary mixtures of CIPbis10BB/6OO8 at various concentrations of the calamitic compound at the relative temperature $\Delta T=-13$ K. Symbols are measured values, solid lines correspond to fits with two relaxations. The small jumps in the curves at $X=0.67$ and 0.92 concentrations are artifacts (due to change in internal sensitivity).

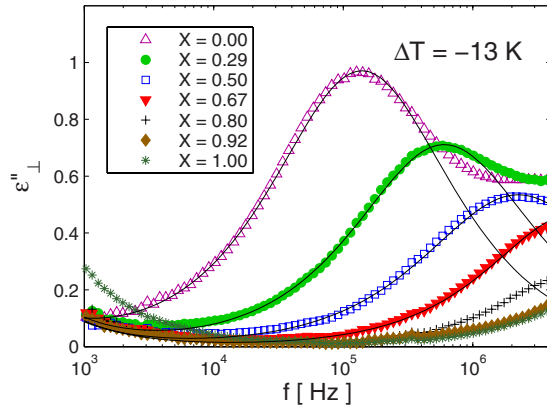


FIG. 9. (Color online) Frequency dependence of the perpendicular component of the loss ε''_{\perp} in the nematic phase of binary mixtures of CIPbis10BB/6OO8 at various concentrations of the calamitic compound at the relative temperature $\Delta T = -13$ K. Symbols are measured values, solid lines correspond to a fit with one relaxation.

12 we present the Arrhenius plot for a selected mixture ($X = 0.5$). The activation energies for the dispersion in the isotropic phase (M_{iso}) was found to be 0.5 eV. In the nematic phase we obtained 0.5 eV for the perpendicular dispersion M_{\perp} , while for the lower frequency $M_{\parallel 1}$ and the higher frequency $M_{\parallel 2}$ dispersions in the parallel component we got 1.6 and 0.8 eV, respectively. In the smectic phase the activation energy of the dispersion $M_{S_{ml}}$ has a fairly high value (1.3 eV). One can notice that E_A of the isotropic relaxation (M_{iso}) is five times lower in the mixture than in the pure bent-core material. For $M_{\parallel 1}$ and $M_{\parallel 2}$ we have found that the activation energies increased significantly compared to those of $B_{\parallel 1}$ and $B_{\parallel 2}$.

Fit parameters of the different relaxations in the case of the mixture with $X=0.5$ molar fraction of 6OO8 at the relative temperature $\Delta T = +5$ K in the isotropic, $\Delta T = -13$ K in the nematic and $\Delta T = -30$ K in the smectic-C phase are collected in Table II. The corresponding activation energies are also presented in Table II.

V. CALCULATIONS OF MOLECULAR DIPOLE MOMENTS

Current theories describing the dielectric properties of nematics—which will be discussed later in Sec. VI—consider the calamitic molecules as rigid uniaxial ellipsoids with one dipole (the net dipole) fixed at an angle β with respect to the long axis. In order to facilitate a comparison of the experimental data with these theories one has to determine the magnitude and direction of the net dipole for the CIPbis10BB too. These properties have been determined by quantum-chemical calculations using the software packages HYPERCHEM 8 and MATLAB R2009.

The CIPbis10BB molecule has altogether seven polar groups related to the Cl-, -COO-, and the -O- bonds. Moreover, the molecule contains numerous sigma bonds, around which parts of the molecule can rotate. Consequently not only the net dipole moment (μ_m) but even the molecular shape (and thus β) depend strongly on the actual conformation of the molecule.

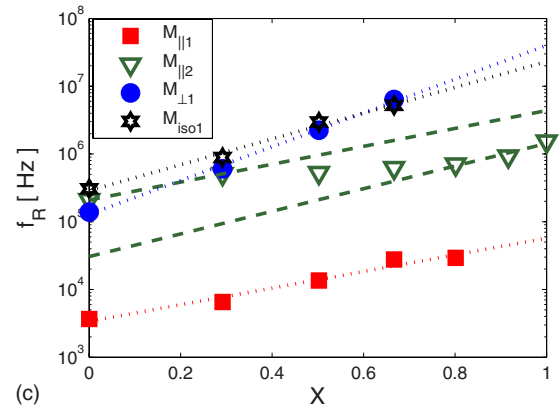
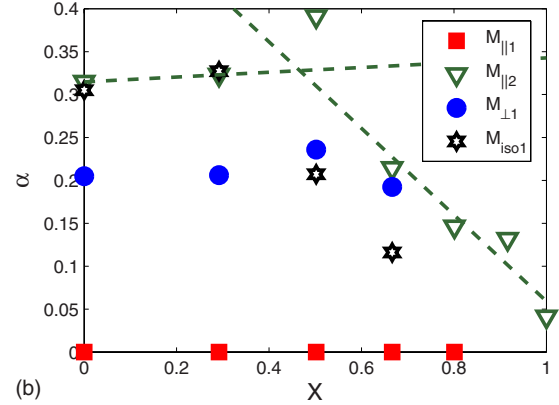
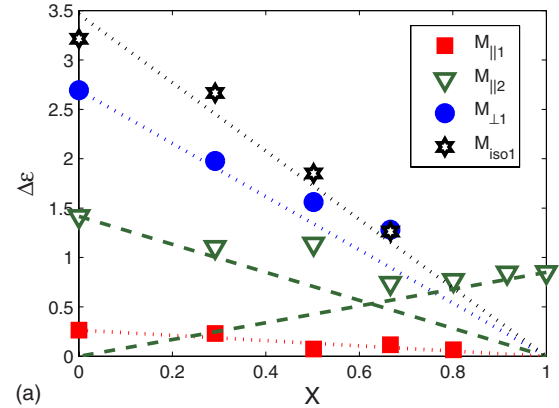


FIG. 10. (Color online) Concentration dependence of the (a) dielectric increments $\Delta\varepsilon$, the (b) symmetric distribution parameters α and the (c) relaxation frequencies f_R in binary mixtures of CIPbis10BB/6OO8 at the relative temperatures $\Delta T = +5$ K and -13 K, in the isotropic and in the nematic phase, respectively. The dotted lines represent linear extrapolations for the concentration dependence. The two dashed lines indicate a decomposition of $M_{\parallel 2}$ into two dispersions explained in the discussion. M refers to the relaxations in mixtures.

Due to the bent-core molecular structure the definition of the long molecular axis is not as trivial as for a rodlike molecule. In order to avoid ambiguity we have taken the eigen-direction belonging to the smallest eigenvalue of the molecular inertial tensor as the longitudinal axis of the bent-core molecule. This definition retains the usual long axis direction for calamitic molecules.

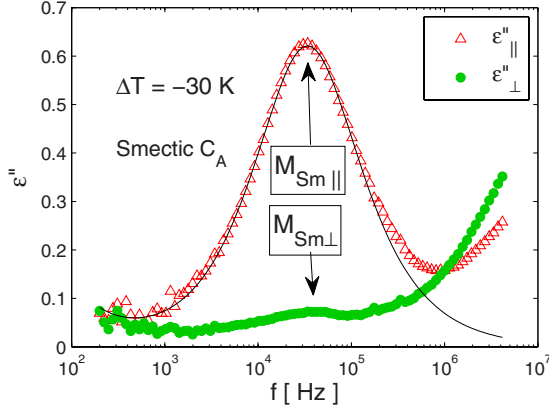


FIG. 11. (Color online) Frequency dependence of the perpendicular and the parallel components of the loss in the SmC_A phase of the mixture with $X=0.5$ at 30 K below T_{Nf} . Symbols are measured values, the solid line corresponds to a fit with one dispersion.

During the quantum mechanical calculation we have pursued the following strategy. After assembling the molecule of CIPbis10BB from the constituting atoms according to the structure in Fig. 1 a molecular geometry optimization has been performed using the Polak-Ribiere conjugate gradient optimization algorithm to find a local energy minimum representing a particular conformer. The molecular properties (e.g., energy, dipole moment, atomic positions) of this conformer have been calculated by the semiempirical quantum-chemical method RM1. From the atomic positions and masses the eigenvalues and eigendirections of the molecular inertial tensor have been determined; then the longitudinal molecular axis has been selected and β has been calculated.

In order to explore the conformation space the following algorithm has been used: in each step random torsions (by random angles in the range of $\pm 60^\circ - 120^\circ$) have been introduced into the molecule at four places, around the four bonds between the oxygen of the carboxyl-group and the carbon of the neighboring benzene ring; then the geometry optimization and the parameter calculations above have been repeated. The algorithm has terminated after 1000 different conformers have been found.

It has turned out that besides the lowest energy conformer there is a manifold of other conformers with an energy dif-

TABLE II. The dielectric increment $\Delta\epsilon$, relaxation frequency f_R , symmetrical distribution parameter α , asymptotic permittivity $\epsilon(\infty)$, and activation energy E_A for the dispersions of the mixture with $X=0.5$ molar fraction of 6OO8 from fits in the isotropic ($\Delta T = +5$ K) in the nematic ($\Delta T = -13$ K) and in the smectic-C ($\Delta T = -30$ K) phase.

Dispersions	$\Delta\epsilon$	f_R (kHz)	α	$\epsilon(\infty)$	E_A (eV)
M_{iso}	1.9	3000	0.2	3.8	0.5
$M_{ 1}$	0.1	14	0	1.6	
$M_{ 2}$	1.1	530	0.4	3.5	0.8
$M_{\perp 1}$	1.6	2200	0.2	4	0.5
$M_{Sm }$	1.5	37	0.1	4.1	1.3

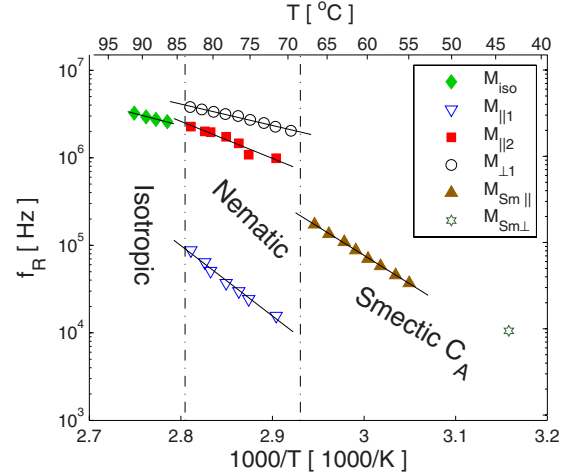


FIG. 12. (Color online) Temperature dependence of the relaxation frequencies in the isotropic, nematic, and smectic phases of the mixture with $X=0.5$ molar fraction of 6OO8 in CIPbis10BB. Symbols are measured values, solid lines correspond to a fit to Eq. (2).

ference less than the thermal energy, however, with considerably different magnitude (3–7 D) and direction (making an angle $\beta \approx 60^\circ - 88^\circ$ with the longitudinal axis) of the molecular dipole moment. As these conformers coexist due to the small energy difference, the net molecular dipole moment could be obtained as a Boltzmann average of the longitudinal and transversal dipole moments of the different conformers at the temperature of $T=360$ K (which corresponds to $\Delta T \approx 10$ K). These calculations yielded $\mu_m = 5.5$ D and $\beta = 74^\circ$ for CIPbis10BB.

We note that earlier calculations on the same compound [9] resulted in considerably smaller (about half as large) μ_m with also a smaller β angle for the most stable conformer of CIPbis10BB which was not compatible with the measured large negative dielectric anisotropy ($\epsilon_a \approx -1.7$). According to the Maier-Meier molecular theory of (calamitic) nematics [12], the sign of ϵ_a should be negative for $\beta > 54.7^\circ$, otherwise it is expected to be positive (assuming that the effect of electronic polarizability anisotropy is neglected). For the CIPbis10BB our quantum-chemical calculations yielded $\beta = 74^\circ$ which is in accordance with the obtained $\epsilon_a < 0$. We believe that the present calculations are more precise due to using a more sophisticated quantum-chemical method (the RM1 instead of the AM1) combined with the averaging over the manifold of conformers.

Similar calculations have been performed for the pure calamitic 6OO8 too at the same temperature of $T=360$ K (which now corresponds to $\Delta T \approx -4$ K) yielding $\mu_m = 2.7$ D and $\beta = 63^\circ$.

VI. DISCUSSION

The induced polarization determining the dielectric permittivity is composed of several contributions, such as: the reorientation of the permanent net dipole moment via the rotation of the molecule as a whole, intramolecular rotation of polar groups, the electronic polarization related to in-

tramolecular deformation of the charge distribution and other, collective motions, such as the Goldstone-mode in the chiral SmC phase [8,13,14]. The general reason for dielectric dispersions is that a given molecular, intramolecular, or collective motion cannot contribute to the macroscopic polarization when the frequency of the exciting electric field exceeds the characteristic frequency of that mode. Electronic polarization modes are usually fast, their relaxations fall into the optical frequency range. Therefore, when analyzing the dielectric behavior below 10 GHz [as we do it in Eq. (1)] we do not consider them.

A. Dispersions in the isotropic phase

The theory for dielectric relaxations in isotropic polar liquids has been derived by Debye assuming spherical molecules with noninteracting dipole moments [15]. Though the predictions of this Debye model do not match experimental results well quantitatively in most of the cases, some of its conclusions still hold qualitatively; namely, larger molecules and/or higher viscosities are expected to reduce the relaxation frequency.

The dielectric increment in isotropic fluids is provided by the Onsager-formula [16] which also assumes spherical molecules with no dipolar interactions,

$$\Delta\varepsilon \frac{3\varepsilon(\infty) + 2\Delta\varepsilon}{(\varepsilon(\infty) + \Delta\varepsilon)(\varepsilon(\infty) + 2)^2} = \frac{N}{9\varepsilon_0 k_B T} \mu_{ons}^2, \quad (3)$$

where N is the number of molecules in unit volume and μ_{ons} is the dipole moment of the molecule.

In the isotropic phase of liquid crystals mostly one dispersion is found at high f , although there exist a few reports about two dispersions [17,18]. In practice Eq. (3) works well quantitatively for calamitics with relatively weak dipoles [19], in spite of the shape anisotropy and the assumption on the lack of interactions between dipole moments. However, for strongly polar materials the Onsager-equation needs an improvement, as pointed out by Kirkwood and Fröhlich. They introduced a correction [20,21] to Eq. (3) in the form

$$\mu_{ons}^2 = \mu_m^2 g, \quad (4)$$

where μ_m is the molecular dipole moment and the factor g describes their interaction. $g=1$ (no interaction) has been found in the isotropic phase of calamitic liquid crystals only for compounds with a relatively small μ_m , while $g < 1$ is often detected for molecules with large dipole moment along their long axis (e.g., cyano biphenyls). This has been interpreted as a preference for antiparallel orientation of neighboring dipoles (corresponding to the minimum of the interaction energy) leading to a reduction of the effective dipole moment compared to μ_m .

In our system in the isotropic phase of the pure calamitic 6O08 and in that of the 6O08 rich ($X > 0.67$) mixtures only the low frequency tail of a high f dispersion could be detected, indicating that most of the dispersion is outside of the frequency range of our measurements. With increasing portion of the bent core component, however, the isotropic relaxation frequency shifts downward to $f_{iso} \approx 300$ kHz in the pure CIPbis10BB as seen in Fig. 10(c). This value is unusu-

ally low for an isotropic dispersion. It can be understood by taking into account that the isotropic viscosity is one to two orders of magnitude larger than the usual values in calamitics [22]. Moreover, the approximately two times bigger size of the BC molecule has an additional significant reducing effect on the relaxation frequency according to the qualitative trends resulting from the Debye theory.

Let us check now the relation between the dielectric increment and the molecular dipole moment using Eq. (3) at a given temperature ($\Delta T = +5$ K). N can be calculated from the molar weight and from the density assumed to be 1000 kg/m^3 . Our experiments indicated that in the isotropic phase of the pure BC compound there are two dispersions, the first one (B_{iso1}) at around 0.3 MHz with $\Delta\varepsilon_{B_{iso1}} = 3.2$ and $\alpha_{B_{iso1}} = 0.3$. If we apply Eq. (3) we obtain an effective dipole moment of 3.6 D, which contributes to the dispersion. This is lower than μ_m , resulting in a value of $g = 0.4$ for the factor of dipole interaction. The second dispersion (B_{iso2}) occurs at higher frequencies (out of our measurement range) with an increment of $\Delta\varepsilon_{B_{iso2}} \approx 1.4$, which we obtained by incorporating all contributions up to the optical frequencies. We attribute this dispersion to intramolecular rotations of the contributing seven polar groups within the molecule. We note, that the complete increment of the two processes, $\Delta\varepsilon_{B_{iso1}} + \Delta\varepsilon_{B_{iso2}} = 4.6$, results in an effective $\mu_{eff} = 5.6$ D which is very near to the calculated μ_m .

B. Dispersions in the nematic phase of the pure compounds

Description of the dielectric behavior of the mesophases clearly requires a different approach than that of the isotropic case. The frequency dependent dielectric phenomena in calamitic compounds are well understood in the frame of a polar rod model which assumes that the molecules are rigid uniaxial ellipsoids with a dipole moment [18,19,23–25]. In most cases one detects three distinguishable dispersions for the (calamitic) nematic phase: two in the parallel orientation, and one in the perpendicular one [8]. The dispersion with the lowest frequency ($C_{||1}$) (C refers to relaxations in calamitics) appears in the parallel component; it is of Debye type and corresponds to the rotation of the molecules around their short axis. The higher frequency parallel dispersion ($C_{||2}$) is a superposition of more than one molecular movements; thus in general, it is of Cole-Cole type. One can link it to the rotational movements around the long axis of the molecule and around the director. The characteristic frequency of the third relaxation (C_{\perp}) which is detectable in the perpendicular component, is usually close to $f_{C||2}$. C_{\perp} is a composite (Cole-Cole) mode too and is interpreted also as the rotation of molecules around their long axis and around the director. The contributions of the three molecular rotations to the dispersions in the parallel and the perpendicular components of the permittivity depend on the magnitude and the orientation of the molecular dipole moment, as well as on the order parameter of the phase.

Our measurements on 6O08 in the parallel component 13 K below the isotropic transition showed $f_{C||1} = 1.5$ MHz with $\alpha_{C||1} = 0.04$ (which indicates a basically Debye-type behavior). This dispersion can clearly be identified as the one re-

TABLE III. The dielectric increment $\Delta\epsilon$, relaxation frequency f_R , symmetrical distribution parameter α , asymptotic permittivity $\epsilon(\infty)$, and activation energy E_A for the dispersions of 6008 at $\Delta T = -13$ K. Literature data for relaxation frequencies of 6008 [26] and of 10006 [27] are also shown.

Dispersions	$\Delta\epsilon$	f_R (MHz)	α	$\epsilon(\infty)$	E_A (eV)
C_{\parallel}	0.85	1.5 (1.6 ^a and 1.8 ^b)	0	2.9	1
$C_{\parallel 2}$		(500 ^b)			
C_{\perp}		(400 ^b)			

^aApproximate value for 6008 at $\Delta T = -10$ K from [26].

^bApproximate values for 10006 at $\Delta T = -4$ K from [27].

lated to the molecular rotation around the short axis. The dispersions $C_{\parallel 2}$ and C_{\perp} are expected to occur at much higher frequencies. Indeed, the beginning of a high f relaxation is detectable both in the parallel and in the perpendicular components.

Earlier dielectric spectroscopy measurements performed on 6008 [26] mainly focused on the dielectric properties of the SmC phase. The few data available for the nematic phase ($f_{C_{\parallel}} \approx 1.6$ MHz at about 10 K below the clearing point) show good agreement with our results.

Unfortunately higher frequency ($f > 10$ MHz) data which could cover the range for $C_{\parallel 2}$ and C_{\perp} are not available in the literature for 6008. Such measurements have, however, been performed [27] in a broad frequency range up to the gigahertz region on a similar compound, 4-n-decyloxyphenyl 4-n-hexyloxybenzoate (10006, also known as DOBHOP). This compound belongs to the same homologous series of mesogens as our calamitic component 6008; the two molecules differ only in the lengths of the apolar alkyl end chains. Therefore one can expect that the dielectric properties of the two mesogens are quite similar (especially since the parities of the number of carbon atoms constituting the end chains are the same). For 10006, the frequencies of the nematic dispersions discussed above were found $f_{C_{\parallel}} \approx 1.8$ MHz (Debye type), $f_{C_{\parallel 2}} \approx 500$ MHz (Cole-Cole type), and $f_{C_{\perp}} \approx 400$ MHz (Cole-Cole type), respectively, at 4 K below the clearing point. Our results agree well also with these.

The parameters available for the calamitic dispersions of 6008 (and of 10006) obtained from our measurements as well as from the literature are summarized in Table III.

Let us now focus on the nematic phase of the pure BC compound. We have to emphasize, that some basic assumptions of the polar rod model do not fulfill in the case of CIPbis10BB. First, the shape of BC molecules is by far not uniaxial, rather it is biaxial. Second, our conformational calculations reported in Sec. V showed that the BC molecule under discussion is not rigid at all. The actual molecular shape strongly depends on the conformation; furthermore, it has got several significantly polar groups that can rotate. Consequently, the net molecular dipole moment is conformation dependent too. These arguments already make the applicability of the polar rod model of calamitic nematics for BC compounds questionable, just as it occurred in the case of

liquid crystalline dimers [28,29]. Third, as the most evident discrepancy, the measurements have proven (see Table I) that the BC compound has five distinguishable dispersions—3 ($B_{\parallel 1}, B_{\parallel 2}, B_{\parallel 3}$) in the parallel and 2 ($B_{\perp 1}, B_{\perp 2}$) in the perpendicular component—in contrast to the 3 ($C_{\parallel}, C_{\parallel 2}, C_{\perp}$) expected for a calamitic nematic. Moreover, some of the dispersions (e.g., $B_{\parallel 1}$) occur in an unusually low frequency range.

We want to note, that most recently a very similar dispersion sequence has been found for another BCN compound [30]. The activation energies for the dispersions in the nematic phase (see Table I) are different enough to conclude, that the relaxation processes behind the dispersions $B_{\parallel 1}, B_{\parallel 2}$, and $B_{\perp 1}$ are different. At present, however, it is yet unclear what type of molecular, intramolecular, or collective motions are responsible for the dispersions observed. Such an identification cannot be done without a reconsideration (or extension) of the polar rod model, which is beyond the scope of the present work.

C. Dispersions in the mixtures

Let us now try to understand the dielectric spectra of the mixtures. Although the molecular shape and size of the two components are significantly different, the system showed full miscibility [11]. Therefore one can safely assume that the bulk properties (such as viscosity, elastic and static electric properties, etc.) of the mixtures change essentially monotonically with the concentration. As an example the static dielectric constant varies roughly linearly versus concentration as it can be deduced from Fig. 8(a). Other physical properties might have a stronger concentration dependence; e.g., the viscosity of the mixtures depends exponentially on the molar fraction of the components which have strongly different viscosities, as it has been reported by Kresse *et al.* [31].

The characteristic frequencies of dispersions are strongly influenced by the properties (e.g., size, dipole moment) of individual molecules, but are also affected by some bulk properties like viscosity (the latter characterizes the local environment for the basically molecular reorientational processes). Based on these arguments we can assume that, as far as the dielectric spectra of the mixtures are concerned, all dispersions belonging to either component may be present simultaneously. This idea of interpreting dispersions in a mixture as a superposition of those of the components have already been arisen in earlier studies on calamitics [31,32]. In calamitic mixtures, however, the relaxation frequencies of the components fall into the same range, therefore the contributions could not be easily separated. In our system the structure of the components as well as the frequency ranges of their dispersion differ largely. In the following we will show that the dielectric spectra of their mixtures [shown before in Figs. 8(b) and 8(c)] can be interpreted using the above assumption, i.e., as a superposition of the BC and calamitic dispersions.

In the isotropic phase, as well as in the perpendicular component of the nematic phase, two dispersions exist for the BC compound and one is expected for the calamitic, however, only one of these three (B_{iso1} and $B_{\perp 1}$, respec-

tively) falls into the measurement frequency range. Indeed, in the mixtures one dispersion (M_{iso} and $M_{\perp 1}$, respectively, see Table II) could be detected experimentally with a dielectric increment roughly proportional to the molar fraction of the BC compound [$\Delta\epsilon_{M_{iso}}, \Delta\epsilon_{M_{\perp 1}} \propto (1-X)$; see the dotted lines in Fig. 10(a)]. Consequently M_{iso} and $M_{\perp 1}$ correspond to (or originate from) B_{iso1} and $B_{\perp 1}$, respectively. It can be seen in Fig. 10(c) that the logarithm of both relaxation frequencies, $f_{M_{iso}}$ and $f_{M_{\perp 1}}$, increases linearly with the molar fraction of the calamitic indicating the influence of a diluted environment. For the highest calamitic contents even these dispersions moved above our frequency range, so $f_{M_{iso}}$ and $f_{M_{\perp 1}}$ could not be determined. The increase in the relaxation frequencies with increasing molar fraction of the calamitic is in agreement with the concentration dependence of the viscosity mentioned above [31].

In the parallel component in the nematic phase three dispersions exist for the BC compound (see Table I) and two for the calamitic (see Table III), however, only three ($B_{\parallel 1}$, $B_{\parallel 2}$ and $C_{\parallel 1}$) of the five fall into the f range of the measurement. Seemingly in the mixtures we could find experimentally two dispersions: $M_{\parallel 1}$ with $\alpha_{M_{\parallel 1}} \approx 0$ and $M_{\parallel 2}$ with a fairly large $\alpha_{M_{\parallel 2}}$ (see Table II). For the lower f dispersion ($M_{\parallel 1}$) the dielectric increment $\Delta\epsilon_{M_{\parallel 1}}$ changes roughly proportionally to the molar fraction of the BC compound [$\Delta\epsilon_{M_{\parallel 1}} \propto (1-X)$; see the dotted line in Fig. 10(a)], while the logarithm of its relaxation frequencies, $f_{M_{\parallel 1}}$ increases linearly with X . These clearly indicate that the dispersion $M_{\parallel 1}$ comes from the BC dispersion $B_{\parallel 1}$. For the mixture with highest calamitic content ($X=0.916$) the dispersion $M_{\parallel 1}$ could not be resolved experimentally, most probably due to its vanishing dielectric increment.

In contrast to the dispersions discussed above, the characteristics of the dispersion $M_{\parallel 2}$ exhibit a different concentration dependence. In Fig. 8(b) it can well be observed, that at medium concentrations the loss peaks called $M_{\parallel 2}$ are flattened. We think that this effect is due to the merging of two different dispersions: one originating from the calamitic and one from the BC compound. Mathematically the sum of two Debye-type relaxations can be equivalent to one Cole-Cole type relaxation if their characteristic frequencies are close to each other, but trivially the decomposition of a composite relaxation cannot be done unambiguously. The α symmetrical distribution parameter is a good indicator of how composite a relaxation is. In Fig. 10(b) the concentration dependence of α shows a maximum at $X=0.5$ molar fraction, which supports our idea.

It can be seen in Fig. 10(c) and in Tables I and III that $f_{B_{\parallel 2}}$ and $f_{C_{\parallel 1}}$ are quite close to each other. Therefore it is not surprising that our CNLS algorithm used to fit the experimental data was not able to distinguish the two dispersions which are not separated well enough in f . We note that the dispersion $B_{\parallel 3}$ with its relaxation frequency lying above the experimental f range already affects the high f region of the spectra, making the picture more complicated mainly at higher concentrations of the BC compound. We also note that under the conditions given even novel separation methods [33] that can magnify the differences between relaxation peaks, however, on the expense of increased noise, has not proven to be efficient.

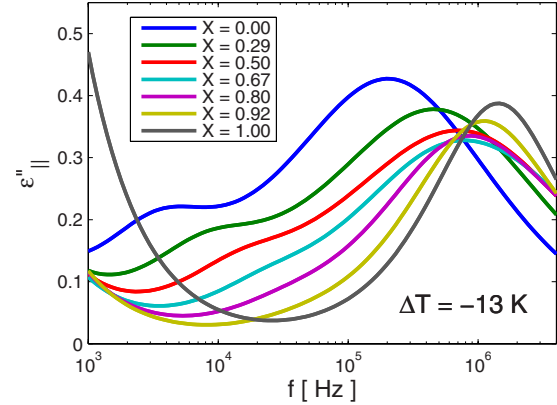


FIG. 13. (Color online) Synthesized dielectric spectrum of the parallel component of the loss for binary mixtures of ClPbis10BB/6O08 assuming three dispersions.

Based on the argument above we propose that $M_{\parallel 2}$ should be interpreted as a superposition of two dispersions, $M_{\parallel 2a}$ and $M_{\parallel 2b}$. $M_{\parallel 2a}$ is related to the BC dispersion $B_{\parallel 2}$ hence its dielectric increment should vary proportionally to the molar fraction of the BC compound [$\Delta\epsilon_{M_{\parallel 2a}} \propto (1-X)$], while $M_{\parallel 2b}$ comes from the calamitic dispersion $C_{\parallel 1}$ hence its dielectric increment should be proportional to the molar fraction of the calamitic ($\Delta\epsilon_{M_{\parallel 2b}} \propto X$); as drawn by dashed lines in Fig. 10(a). For the concentration dependence of the relaxation frequencies and that of α we take a linear extrapolation from the values of the pure compounds and that of the closest mixture, i.e., from $X=0$ and $X=0.29$ for $M_{\parallel 2a}$ and from $X=1$ and $X=0.92$ for $M_{\parallel 2b}$. These are depicted as the dashed lines in Figs. 10(c) and 10(b). The dielectric spectra of the mixtures can then be synthesized as a superposition taking the extrapolated values for $M_{\parallel 2a}$ and $M_{\parallel 2b}$, and the experimentally fitted ones for $M_{\parallel 1}$ and the dc conductivity. Figure 13 shows this synthesized spectra for our mixtures which reflects convincingly all features of the experimental spectra in Fig. 8(b) apart from the lack of the high f distortions (the contribution from dispersions above the measurement f range were not included into the superposition).

VII. SUMMARY

Dielectric spectroscopy measurements in the range of 200 Hz and 4 MHz have been performed on a mono-chloro substituted bent-core nematic liquid crystal and on its binary mixtures with a calamitic nematic. In the pure bent-core compound we have detected more relaxations, than usual in calamitic nematic materials. All detected dispersions in the pure BCN including those in the isotropic phase occur at significantly lower frequencies than in the calamitic. We find especially interesting the relaxation detected at a few kilohertz. The dispersions measured in the mixtures can be interpreted as the superposition of the modes in the bent-core and calamitic compounds. In order to relate the dielectric increments with the molecular dipole moments we have applied a sophisticated conformational calculation for a large flexible mesogen molecule with numerous polar groups.

Presently no complete theoretical description of the physical phenomena behind the detected dispersions is available

for the bent-core compound. Rotations of the molecular net dipole moment as a whole at lower frequencies as well as intramolecular rotations of the constituent polar groups within the flexible molecule at high frequencies should surely contribute. Nevertheless we cannot exclude the existence of collective modes. Our preliminary calculations show that ferroelectric tilted smectic clusters can induce a Debye-type relaxation in the low frequency region. Some recent measurements [7,22,34] provide indications on the existence of such clusters.

ACKNOWLEDGMENTS

The authors are grateful to K. Fodor-Csorba, J. Williams, and R. Twieg for providing compounds for the measurements, and to S. Pekker for useful discussions on the dipole calculations. Financial support by the Hungarian Research Funds OTKA Grants No. K61075 and No. K81250 and the NSF Grant No. DMR-0606160 are gratefully acknowledged.

-
- [1] H. Takezoe and Y. Takanishi, *Jpn. J. Appl. Phys., Part 1* **45**, 597 (2006).
- [2] J. Harden, B. Mbang, N. Éber, K. Fodor-Csorba, S. Sprunt, J. T. Gleeson, and A. Jákli, *Phys. Rev. Lett.* **97**, 157802 (2006).
- [3] D. B. Wiant, J. T. Gleeson, N. Éber, K. Fodor-Csorba, A. Jákli, and T. Tóth-Katona, *Phys. Rev. E* **72**, 041712 (2005).
- [4] S. Tanaka, H. Takezoe, N. Éber, K. Fodor-Csorba, A. Vajda, and Á. Buka, *Phys. Rev. E* **80**, 021702 (2009).
- [5] P. Tadapatri, U. S. Hiremath, C. V. Yelamaggad, and K. S. Krishnamurthy, *J. Phys. Chem. B* **114**, 10 (2010).
- [6] M. Majumdar, K. Neupane, J. T. Gleeson, A. Jakli, S. Sprunt, Flexoelectric effect in a bent-core liquid crystal measured by Dynamic Light Scattering, Abstract: W8.00006, APS March meeting, New Orleans, 2008 (unpublished).
- [7] O. Francescangeli, V. Stanic, S. I. Torgova, A. Strigazzi, N. Scaramuzza, C. Ferrero, I. P. Dolbnya, T. M. Weiss, R. Bernardi, L. Muccioli, S. Orlandi, and C. Zannoni, *Adv. Funct. Mater.* **19**, 2592 (2009).
- [8] H. Kresse, in *Physical Properties of Liquid Crystals: Nematics*, edited by D. A. Dunmur, A. Fukuda, and G. R. Luckhurst (Inspec, London, 2001), pp. 277–287.
- [9] K. Fodor-Csorba, A. Vajda, G. Galli, A. Jákli, D. Demus, S. Holly, and E. Gács-Báitz, *Macromol. Chem. Phys.* **203**, 1556 (2002).
- [10] D. Wiant, S. Stojadinovic, K. Neupane, S. Sharma, K. Fodor-Csorba, A. Jákli, J. T. Gleeson, S. Sprunt, *Phys. Rev. E* **73**, 030703(R) (2006).
- [11] G. G. Nair, C. A. Bailey, S. Taushanoff, K. Fodor-Csorba, A. Vajda, Z. Varga, A. Bóta, and A. Jákli, *Adv. Mater.* **20**, 3138 (2008).
- [12] W. Maier, G. Meier, *Z. Naturforsch. A*, **16a**, 262 (1961).
- [13] N. E. Hill, Worth E. Vaughan, A. H. Price, and M. Davies, *Dielectric Properties and Molecular Behaviour* (Van Nostrand Reinhold, London, New York, 1969).
- [14] T. Carlsson, B. Zeks, C. Filipic, and A. Levstik, *Phys. Rev. A* **42**, 877 (1990).
- [15] P. Debye, *Polar Molecules* (Reinhold Publishing Corp., New York, 1929), Chap. 5.
- [16] L. Onsager, *J. Am. Chem. Soc.* **58**, 1486 (1936).
- [17] F. Gouda, S. T. Lagerwall, K. Skarp, B. Stebler, F. Kremer, S. Vallerien, *Liq. Cryst.* **17**, 367 (1994).
- [18] A. H. Price and Á. Buka, in *Advances in Liquid Crystal Research and Applications*, edited by L. Bata (Pergamon Press, Akadémiai Kiadó, New York, Budapest (1980), p. 267.
- [19] Á. Buka, P. G. Owen, and A. H. Price, *Mol. Cryst. Liq. Cryst.* **51**, 295 (1979).
- [20] J. G. Kirkwood, *J. Chem. Phys.* **7**, 911 (1939).
- [21] H. Fröhlich, *Theory of Dielectrics* (Oxford University Press, London, 1958).
- [22] C. Bailey, K. Fodor-Csorba, J. T. Gleeson, S. N. Sprunt, and A. Jakli, *Soft Matter* **5**, 3618 (2009).
- [23] J. McConnell, *Rotational Brownian Motion and Dielectric Theory* (Academic Press, New York, 1980).
- [24] L. Bata and Á. Buka, *Acta Phys. Pol.* **A54**, 635 (1978).
- [25] W. T. Coffey and Yu. P. Kalmykov, *Adv. Chem. Phys.* **113**, 487 (2000).
- [26] C. Druon and J. M. Wacrenier, *Mol. Cryst. Liq. Cryst.* **108**, 291 (1984).
- [27] Á. Buka and L. Bata, *Advances in Liquid Crystal Research and Applications*, edited by L. Bata (Pergamon Press, Akadémiai Kiadó, New York, Budapest (1980), p. 261.
- [28] D. A. Dunmur, G. R. Luckhurst, M. R. de la Fuente, S. Diez, and M. A. Pérez Jubindo, *J. Chem. Phys.* **115**, 8681 (2001).
- [29] M. Stocchero, A. Ferrarini, G. J. Moro, D. A. Dunmur, and G. R. Luckhurst, *J. Chem. Phys.* **121**, 8079 (2004).
- [30] P. Tadapatri, U. S. Hiremath, C. V. Yelamaggad, and K. S. Krishnamurthy, *J. Phys. Chem. B* **114**, 1745 (2010).
- [31] H. Kresse, U. Schuhmacher, D. Demus, and W. Schäfer, *Mol. Cryst. Liq. Cryst.* **170**, 1 (1989).
- [32] L. Bata and G. Molnár, *Chem. Phys. Lett.* **33**, 535 (1975).
- [33] K. Merkel, A. Kocot, J. K. Vij, G. H. Mehl, and T. Meyer, *Phys. Rev. E* **73**, 051702 (2006).
- [34] V. Domenici, T. Apih, and C. A. Veracini, *Thin Solid Films* **517**, 1402 (2008).